

## COMMUNICATION

## Aziridinium Cation Templating 3D Lead Halide Hybrid Perovskites

Hanna R. Petrosova,<sup>a</sup> Olesia I. Kucheriv,<sup>a</sup> Sergiu Shova<sup>b</sup> and Il'ya A. Gural'skiy<sup>\*a</sup>Received 00th January 20xx,  
Accepted 00th January 20xx

DOI: 10.1039/x0xx00000x

**This paper describes a synthesis of the first aziridinium-based compounds, namely hybrid perovskites (AzrH)PbHal<sub>3</sub> (where AzrH = aziridinium, Hal = Cl, Br or I). This highly reactive species was stabilized in 3D lead halide frameworks and was found to be enough small organic cation to promote a formation of semiconducting organo-inorganic materials.**

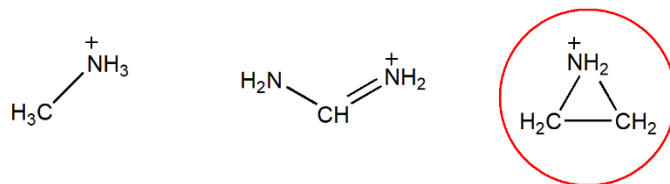
As for today, there is a considerable attention to hybrid perovskites, the origin of which is mostly their potential for photovoltaic application.<sup>1</sup> Moreover, they show perspectives as materials for production of lasers,<sup>2,3</sup> light emitting diodes,<sup>4,5</sup> photodetectors,<sup>6,7</sup> for memory storage,<sup>8,9</sup> water splitting,<sup>10,11</sup> etc.

Hybrid lead halide perovskites have general formula A<sup>+</sup>PbHal<sub>3</sub><sup>-</sup>, where A<sup>+</sup> is an organic cation and Hal<sup>-</sup> is a halogen anion. For today, the most studied and applied is MAPbI<sub>3</sub> (MA = methylammonium). This compound is a semiconductor with the bandgap of 1.5-1.6 eV and it displays characteristics which are necessary for an active layer in an efficient solar cell: high absorption coefficient, long carrier diffusion length and high carrier mobility.<sup>1</sup> MAPbHal<sub>3</sub> was firstly used for photovoltaic applications in 2009.<sup>12</sup> This led to the creation of a new class of solar cells based upon hybrid perovskites, among which, notably, only 3D lead halide hybrid perovskites display attractively high conversion rates. Replacement of MA by FA (FA = formamidinium) allowed to obtain FAPbI<sub>3</sub> perovskite with slightly lower bandgap which allows absorption of photons over a broader spectral range.<sup>13</sup> Partial substitution of iodine by bromine has been performed for both MA<sup>14,15</sup> and FA<sup>16,17</sup> lead

perovskites and allowed to shift the bandgap gradually in the range of approximately 1.5-2.3 eV. Recently, the highest efficiency of 25.2% was reached with a solar cell based on 3D hybrid perovskite with mixed MA/FA cation and mixed I/Br anion composition.<sup>18</sup>

On the other hand, from the synthetic point of view there is scarces set of available 3D lead halide hybrid perovskites. This is because of strict criteria to the selection of cations that can be used for the design of these highly desirable frameworks. The selection of universal organic cations is limited to very small cations like MA and FA (see Scheme 1), while other (mainly larger) species like ethylammonium already promote the creation of 2D layered<sup>19-22</sup> or 1D chained lead halide perovskites.<sup>23</sup> Azitidinium (a 4-membered cycle) is also too large to form cubic 3D perovskites as a sole cation.<sup>24-26</sup> Worth noting that methylhydrazonium can form CH<sub>3</sub>NH<sub>2</sub>NH<sub>2</sub>PbCl<sub>3</sub> and CH<sub>3</sub>NH<sub>2</sub>NH<sub>2</sub>PbBr<sub>3</sub> 3D perovskites<sup>27</sup> and fluoromethylammonium can form FCH<sub>2</sub>NH<sub>3</sub>PbBr<sub>3</sub> 3D perovskite<sup>28</sup>.

A small enough cation can be potentially obtained via protonation of aziridine, a three-membered heterocycle bearing one nitrogen atom in the cycle (Scheme 1). Due to the ring strain of aziridine it is a highly reactive substrate in nucleophilic ring opening reactions.<sup>29</sup> This potential cation is unstable and to the best of our knowledge was never isolated in any salt before. On the other hand, aziridinium cation is theoretically considered as an excellent template for the formation of 3D lead halide hybrid perovskites for perspective applications.<sup>30,31</sup>



**Scheme 1.** Organic cations that are known to form Cl, Br and I 3D lead halide hybrid perovskites (methylammonium, formamidinium) and the aziridinium cation that was used in the present work.

<sup>a</sup> Department of Chemistry, Taras Shevchenko National University of Kyiv, Volodymyrska St. 64, Kyiv 01601, Ukraine  
E-mail: [illia.gural'skiy@univ.kiev.ua](mailto:illia.gural'skiy@univ.kiev.ua)

<sup>b</sup> Department of Inorganic Polymers, Petru Poni Institute of Macromolecular Chemistry, Aleea Grigore Ghica Voda 41-A, Iasi 700487, Romania

Electronic Supplementary Information (ESI) available: synthetic procedures, physical characterization details, IR spectra, PXRD patterns, TGA curves, crystallographic tables. See DOI: 10.1039/x0xx00000x

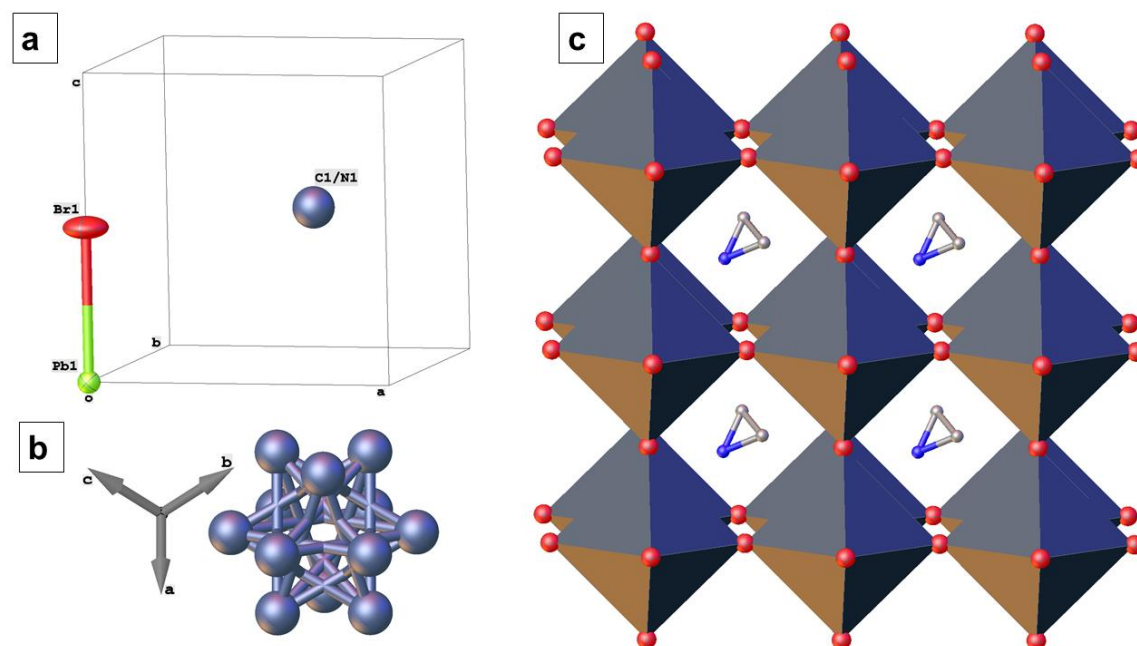


**Figure 1.** Crystal structure of  $(\text{AzrH})\text{PbHal}_3$  (Hal = Cl, Br, I). (a) Crystallographically independent part that includes one Pb site, one Hal site and one site shared by disordered C and N atoms. (b) Modelled disorder of the aziridinium cation. (c) 3D anionic haloplumbate framework build of corner-connected  $\text{PbBr}_6$  polyhedra, while aziridinium occupies cationic positions.

In this paper we report on the synthesis of perovskites  $(\text{AzrH})\text{PbHal}_3$  (where AzrH = aziridinium, Hal = Cl, Br or I) where this unique cation is not only stable but also is an efficient template for building 3D perovskite structures.  $(\text{AzrH})\text{PbHal}_3$  were synthesized via reactions between acidic solutions of lead halides and aziridine. Our attempts to firstly prepare a solution of aziridinium salt ended up with a predictable cycle opening; e.g., a formation of low dimensionality perovskites based upon 2-iodoethylammonium cation was observed (they are already known from literature<sup>32</sup>). On the other hand, when aziridinium salt is formed *in situ* and immediately reacts with lead halide, the desired compounds are formed (see ESI for the experimental details). The key point of the experimental success here is a direct formation of a perovskite structure which hosts the reactive cation and preserves it from further reactions.

**Table 1.** Structural and optical characteristics of  $(\text{AzrH})\text{PbHal}_3$  (293 K).

Compound	$(\text{AzrH})\text{PbCl}_3$	$(\text{AzrH})\text{PbBr}_3$	$(\text{AzrH})\text{PbI}_3$
Space group	$Pm\bar{3}m$	$Pm\bar{3}m$	$Pm\bar{3}m$
a (Å)	5.7610(2)	5.9739(3)	6.3640(4)
Pb–Hal (Å)	2.8805(1)	2.9870(2)	3.1820(2)
N1–H...Hal1 (Å)	3.23(2)	3.40(3)	3.69(1)
C1–C1/N1 (Å)	1.45(4)	1.43(3)	1.40(2)
Optical bandgap (eV)	2.99	2.27	1.52

Single crystals of perovskites were obtained via reaction of lead halide with aziridine in acidic media (Cl and Br perovskites) or through slow vapor diffusion of aziridine (I perovskite) (see ESI for experimental details). The structures of all three perovskites were studied via single crystal X-ray diffraction. At 293 K they all crystallize in the cubic lattice system, space group  $Pm\bar{3}m$ .<sup>‡</sup> Crystallographically independent part includes one Pb site, one Hal site and one site shared by disordered C and N atoms. The frameworks are built of ideal  $\text{PbHal}_6$  octahedra (Hal–Pb–Hal = 90°) that are bound through corner sharing (Figure 1c). Cell parameters and Pb–Hal bond lengths are summarized in Table 1. Cell parameter *a* corresponds to the nearest Pb...Pb distance, i.e., defined by the Pb–Hal bond length (Figure 1a). It progressively grows in the row Cl < Br < I in line with the atomic radii of halogens (Table 1).

Geometries of the haloplumbate frameworks are similar to those with Cs, MA and FA cations, showing only minor effects of the cations on the anionic architecture (see Table S1 in the ESI). The cationic positions are occupied by a highly disordered aziridinium cation. It can be modeled as disordered between 36 positions (Figure 1b) with C–C/N bond lengths of 1.40–1.45 Å. But considering a very low scattering from the cation comparing to the  $[\text{PbHal}_3]$  framework, similar scattering from C and N atoms, and because of the high cubic symmetry of these compounds, this rather should be considered as just one of many possible ways to model this disorder. Aziridinium cation displays short contacts with halogens of the anion framework, namely N1–Hal distances are 3.23 Å (Cl), 3.40 Å (Br) and 3.69 Å (I) that corresponds to the presence of hydrogen bonding between the cationic and the anionic parts.

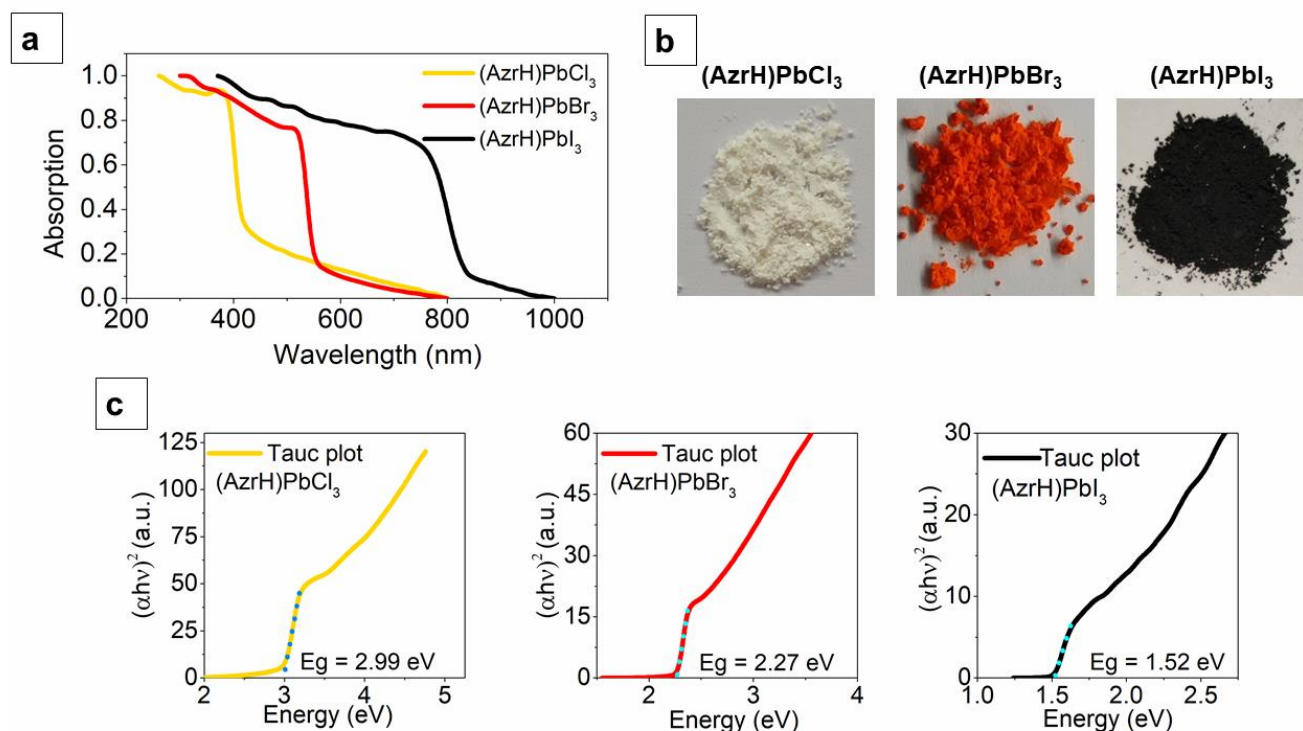


**Figure 2.** (a) Normalized optical absorption spectra of (AzrH)PbHal<sub>3</sub> (Hal = Cl, Br, I). (b) Photographs of (AzrH)PbHal<sub>3</sub>. (c) Tauc plots for the three perovskites showing optical bandgaps

PXRD patterns show the presence of only one described cubic phase for all perovskites (Figures S1-S3, ESI). Re-measurements after c.a. 1.5 months confirmed its good stability, while the appearance of minor impurities is detected for (AzrH)PbI<sub>3</sub> (Figures S4-S6, ESI). TGA confirm no considerable mass loss for these perovskites until c.a. 300 °C (Figure S7, ESI).

Optical absorption spectra of (AzrH)PbHal<sub>3</sub> are shown in Figure 2a. They all display a typical absorption for semiconducting materials, namely an abrupt drop of the absorption at certain wavelength: 420 nm (Cl), 553 nm (Br) and 830 nm (I). This originates from a bandgap that lays in the visible (Cl and Br perovskites) or NIR regions (I perovskite). This explains the colors of new perovskites, which are colorless (Cl), orange (Br) and black (I) (Figure 2b).

Building Tauc plots from absorption spectra is a classic approach to extract the values of optical bandgaps. Tauc plots for the three perovskites are given in Figure 2c and bandgaps of 2.99 eV (Cl), 2.27 eV (Br) and 1.52 eV (I) were determined. Notably the determined values are very close to those of perovskites with Cs, MA and FA cations (see Table S2 in ESI for comparison). This confirms the predominant role of a cation in driving the formation of 3D haloplumbate frameworks, and this 3D architecture mostly defines properties of perovskites.

A special attention should be paid to the (AzrH)PbI<sub>3</sub> perovskite whose optical absorption covers the whole visible range making it the most perspective for photovoltaic applications and photodetection. Notably while structural and optical properties of this perovskite are similar to those with other cations, a different nature of the cation may affect the charge mobilities which are crucial for these compounds

In conclusion, we have observed a nice interplay when, from one hand, a small aziridinium cation stabilizes practically attractive 3D perovskite structure and, on the other hand, a perovskite framework hosts and stabilizes the aziridinium cation. While (AzrH)PbI<sub>3</sub> can be considered as a perspective photovoltaic material, other perovskites (namely of Sb, Sn, Bi, Ge) based on the aziridinium cation should be a matter of further design. A following work should be done towards thin films of these perovskites, since deposition from polar solvents (like DMF or DMSO) is poorly suitable for these compounds of the highly reactive aziridinium cation.

Authors acknowledge the financial support from the Ministry of Education and Science of Ukraine (grant 22BF037-09) and the courage of Armed Forces of Ukraine that made the submission of this manuscript possible.

## Notes and references

‡ CCDC deposition numbers 2153152-2153154.

- 1 J. Y. Kim, J. W. Lee, H. S. Jung, H. Shin and N. G. Park, *Chem. Rev.*, 2020, **120**, 7867–7918.
- 2 Z. Huang, C. Yin, Y. Hong, H. Li, K. Hong, T. S. Kao, M. Shih and T. Lu, *Adv. Opt. Mater.*, 2021, **9**, 2100299.
- 3 N. Zhang, Y. Fan, K. Wang, Z. Gu, Y. Wang, L. Ge, S. Xiao and Q. Song, *Nat. Commun.*, 2019, **10**, 1770.
- 4 Y. Cao, N. Wang, H. Tian, J. Guo, Y. Wei, H. Chen, Y. Miao, W. Zou, K. Pan, Y. He, H. Cao, Y. Ke, M. Xu, Y. Wang, M. Yang, K. Du, Z. Fu, D. Kong, D. Dai, Y. Jin, G. Li, H. Li, Q. Peng, J. Wang and W. Huang, *Nature*, 2018, **562**, 249–253.
- 5 M. Lu, Y. Zhang, S. Wang, J. Guo, W. W. Yu and A. L.

- Rogach, *Adv. Funct. Mater.*, 2019, **29**, 1902008.
- 6 Y. Peng, X. Liu, Z. Sun, C. Ji, L. Li, Z. Wu, S. Wang, Y. Yao, M. Hong and J. Luo, *Angew. Chemie Int. Ed.*, 2020, **59**, 3933–3937. 28
- 7 Z. Xu, W. Weng, Y. Li, X. Liu, T. Yang, M. Li, X. Huang, J. Luo and Z. Sun, *Angew. Chemie Int. Ed.*, 2020, **59**, 21693–21697. 29
- 8 Y. Zhang, S. Poddar, H. Huang, L. Gu, Q. Zhang, Y. Zhou, S. Yan, S. Zhang, Z. Song, B. Huang, G. Shen and Z. Fan, *Sci. Adv.*, 2021, **7**, 1–11. 30
- 9 S. Kim, J. Yang, E. Choi and N. Park, *Adv. Funct. Mater.*, 2020, **30**, 2002653. 31
- 10 K. Ren, S. Yue, C. Li, Z. Fang, K. A. M. Gasem, J. Leszczynski, S. Qu, Z. Wang and M. Fan, *J. Mater. Chem. A*, 2022, **10**, 407–429. 32
- 11 E. Edwardes Moore, V. Andrei, S. Zacarias, I. A. C. Pereira and E. Reisner, *ACS Energy Lett.*, 2020, **5**, 232–237.
- 12 Kojima, A, T. K, Shirai, Y, Miyasaka and T, *J. Am. Chem. Soc.*, 2009, **131**, 6050–6051.
- 13 N. J. Jeon, J. H. Noh, W. S. Yang, Y. C. Kim, S. Ryu, J. Seo and S. Il Seok, *Nature*, 2015, **517**, 476–480.
- 14 A. Sadhanala, F. Deschler, T. H. Thomas, S. E. Dutton, K. C. Goedel, F. C. Hanusch, M. L. Lai, U. Steiner, T. Bein, P. Docampo, D. Cahen and R. H. Friend, *J. Phys. Chem. Lett.*, 2014, **5**, 2501–2505.
- 15 S. Aharon, B. El Cohen and L. Etgar, *J. Phys. Chem. C*, 2014, **118**, 17160–17165.
- 16 G. E. Eperon, S. D. Stranks, C. Menelaou, M. B. Johnston, L. M. Herz and H. J. Snaith, *Energy Environ. Sci.*, 2014, **7**, 982.
- 17 T. Jesper Jacobsson, J.-P. Correa-Baena, M. Pazoki, M. Saliba, K. Schenk, M. Grätzel and A. Hagfeldt, *Energy Environ. Sci.*, 2016, **9**, 1706–1724.
- 18 D.-Y. Son, J.-W. Lee, Y. J. Choi, I.-H. Jang, S. Lee, P. J. Yoo, H. Shin, N. Ahn, M. Choi, D. Kim and N.-G. Park, *Nat. Energy*, 2016, **1**, 16081.
- 19 S. Wang, X. Liu, L. Li, C. Ji, Z. Sun, Z. Wu, M. Hong and J. Luo, *J. Am. Chem. Soc.*, 2019, **141**, 7693–7697.
- 20 B. Luo, Y. Guo, X. Li, Y. Xiao, X. Huang and J. Z. Zhang, *J. Phys. Chem. C*, 2019, **123**, 14239–14245.
- 21 M. Geselle and H. Fuess, *Zeitschrift für Krist. - New Cryst. Struct.*, 1997, **212**, 241–242.
- 22 L. Mao, Y. Wu, C. C. Stoumpos, B. Traore, C. Katan, J. Even, M. R. Wasielewski and M. G. Kanatzidis, *J. Am. Chem. Soc.*, 2017, **139**, 11956–11963.
- 23 J. Im, J. Chung, S. Kim and N. Park, *Nanoscale Res. Lett.*, 2012, **7**, 353.
- 24 S. R. Pering, W. Deng, J. R. Troughton, P. S. Kubiak, D. Ghosh, R. G. Niemann, F. Brivio, F. E. Jeffrey, A. B. Walker, M. S. Islam, T. M. Watson, P. R. Raithby, A. L. Johnson, S. E. Lewis and P. J. Cameron, *J. Mater. Chem. A*, 2017, **5**, 20658–20665.
- 25 J. Tian, D. B. Cordes, C. Quarti, D. Beljonne, A. M. Z. Slawin, E. Zysman-Colman and F. D. Morrison, *ACS Appl. Energy Mater.*, 2019, **2**, 5427–5437.
- 26 J. Tian, D. B. Cordes, A. M. Z. Slawin, E. Zysman-Colman and F. D. Morrison, *Inorg. Chem.*, 2021, **60**, 12247–12254.
- 27 M. Mączka, A. Gągor, J. K. Zaręba, D. Stefanska, M. Drozd, S. Balciunas, M. Šimėnas, J. Banys and A. Sieradzki, *Chem. Mater.*, 2020, **32**, 4072–4082.
- S. Huang, P. Huang, L. Wang, J. Han, Y. Chen and H. Zhong, *Adv. Mater.*, 2019, **31**, 1903830.
- X. E. Hu, *Tetrahedron*, 2004, **60**, 2701–2743.
- Q. Teng, T. Shi, C. Liao and Y.-J. Zhao, *J. Mater. Chem. C*, 2021, **9**, 982–990.
- C. Zheng and O. Rubel, *J. Phys. Chem. Lett.*, 2018, **9**, 874–880.
- S. Sourisseau, N. Louvain, W. Bi, N. Mercier, D. Rondeau, F. Boucher, J.-Y. Buzaré and C. Legein, *Chem. Mater.*, 2007, **19**, 600–607.